Published in final edited form as:
Clin Cancer Res. 2009 March 1; 15(5): 1730–1740. doi:10.1158/1078-0432.CCR-08-2008.

Oncolytic Adenoviral Mutants with E1B19K Gene Deletions Enhance Gemcitabine-induced Apoptosis in Pancreatic Carcinoma Cells and Anti-Tumor Efficacy *In vivo*

Stephan Leitner[1], **Katrina Sweeney**[1], **Daniel Öberg**[1], **Derek Davies**[2], **Enrique Miranda**[1], **Nick R. Lemoine**[1], and **Gunnel Halldén**[1]

[1]Centre for Molecular Oncology and Imaging, Institute of Cancer, Barts and the London School of Medicine and Dentistry, Queen Mary University of London

[2]FACS Laboratory, London Research Institute, Cancer Research UK, Lincolns Inn Fields, London, United Kingdom

Abstract

Purpose—Pancreatic adenocarcinoma is a rapidly progressive malignancy that is highly resistant to current chemotherapeutic modalities and almost uniformly fatal.We show that a novel targeting strategy combining oncolytic adenoviral mutants with the standard cytotoxic treatment, gemcitabine, can markedly improve the anticancer potency.

Experimental Design—Adenoviral mutants with the E1B19K gene deleted with and without *E3B* gene expression (AdΔE1B19K and *dl*337 mutants, respectively) were assessed for synergistic interactions in combination with gemcitabine. Cell viability, mechanism of cell death, and antitumor efficacy *in vivo* were determined in the pancreatic carcinoma cells PT45 and Suit2, normal human bronchial epithelial cells, and in PT45 xenografts.

Results—The ΔE1B19K-deleted mutants synergized with gemcitabine to selectively kill cultured pancreatic cancer cells and xenografts *in vivo* with no effect in normal cells. The corresponding wild-type virus (Ad5) stimulated drug-induced cell killing to a lesser degree. Gemcitabine blocked replication of all viruses despite the enhanced cell killing activity due to gemcitabine-induced delay in G_1/S-cell cycle progression, with repression of cyclin E and cdc25A, which was not abrogated by viral E1A-expression. Synergistic cell death occurred through enhancement of gemcitabine-induced apoptosis in the presence of both AdΔE1B19K and *dl*337 mutants, shown by increased cell membrane fragmentation, caspase-3 activation, and mitochondrial dysfunction.

Conclusions—Our data suggest that oncolytic mutants lacking the antiapoptotic *E1B19K* gene can improve efficacy of DNA-damaging drugs such as gemcitabine through convergence on cellular apoptosis pathways.These findings imply that less toxic doses than currently practicedin the clinic could efficiently target pancreatic adenocarcinomas when combined with adenoviral mutants.

Requests for reprints: Gunnel Halldén, Centre for Molecular Oncology and Imaging, Institute of Cancer, Barts and the London School of Medicine and Dentistry, Queen Mary University of London, London, EC1M 6BQ, UK. Phone: 44-0-207-014-0426; Fax: 44-0-207-014-0431; g.hallden@qmul.ac.uk..

Disclosure of Potential Conflicts of Interest No potential conflicts of interest were disclosed.

Note: Supplementary data for this article are available at Clinical Cancer Research Online (http://clincancerres.aacrjournals.org/).

Europe PMC Funders Author Manuscripts

Adenocarcinoma of the pancreas is always aggressive, with a poor prognosis and few treatment options, and is currently among the leading causes of cancer-related deaths globally (1). Treatments with radiation therapy and chemotherapy have negligible effects with limited improvements in survival using gemcitabine, the current therapy of choice (2). The poor prognosis necessitates the development of novel treatment strategies for this incurable malignancy.

Replication-selective oncolytic viruses represent a novel anticancer approach with proven efficacy in both cancer cells in culture and in tumor xenografts in vivo (3). Extensive data from clinical trials with several selectively replicating adenoviral mutants showed overall safety and tumor selectivity (3–5). One of these mutants, dl1520 (Onyx-015), was the first clinical application designed to complement nonfunctional p53 in tumor cells, later found also to complement the altered mRNA export functions present in many cancers (4, 5). A similar mutant, H101, is now licensed for anticancer therapy in China (Shanghai Sunway Biotech). Although safety and selectivity were verified in numerous trials and patients with both mutants, low efficacy was reported when administered alone. Combination treatments with cytotoxic drugs such as cisplatin and fluorouracil improved efficacy in phase II and III trials with recurrent squamous cell carcinomas of the head and neck (6, 7). Similarly in phase I/II trials targeting pancreatic cancers, no tumor regression was observed when the dl1520 mutant was administered alone (8, 9). However, minor responses and stable disease were reported in combination with gemcitabine.

Various oncolytic mutants with improved potency have been developed such as deletion mutants complementing pRb-pathway alterations (10, 11) and tissue-specific promoterdriven mutants targeting prostate cancer (12, 13) or the majority of solid tumors (14, 15). Pancreatic adenocarcinoma shows prevalent genetic alterations in the pRb, cell cycle, and cell death pathways, making it a suitable target for the more recently developed potent pRb-functional mutants (dl922-947, ref. 10; Ad5Δ24, ref. 11) with potential for highly improved clinical outcomes. In preclinical models, cell killing was reported superior to the dl1520 mutant, whereas tumor selectivity was less specific with replication in cycling normal cells. Consequently, further modifications are necessary to improve on tumor selectivity as well as efficacy in combination with cytotoxic therapies.

The viral antiapoptotic gene E1B19K has been suggested as a potential candidate gene for deletion in already potent replication-selective complementation mutants to minimize toxicity in normal cells (16–18). E1B19K, a functional Bcl-2 homologue, directly binds Bax and Bak-inhibiting oligomerization and mitochondrial pore-formation to block apoptosis (19, 20). The biological function of E1B19K is to inhibit death receptor–induced signaling by preventing Bax-Bak association and enable viral replication and spread. E1B19K also inhibits intrinsically induced apoptosis (both p53-dependent and p53-independent), for example in response to viral E1A proteins or cytotoxic drugs (17, 18, 21–23). In contrast, E1B55K mainly inhibits p53-dependent pathways. We previously showed lower toxicity to normal cells in culture and liver tissue in vivo for adenoviral type 5 (Ad5) and type 2 (Ad2) mutants with the E1B19K gene deleted (16, 24). Antitumor potency was still retained and even enhanced as previously reported for this deletion (25). In all previous studies, however, additional viral genes were deleted such as the E1B55K and E3B genes, and the effects of a single E1B19K deletion had not yet been determined in combinations with cytotoxic drugs. In previous studies we showed that retaining the E3B genes could significantly improve in vivo efficacy by delaying viral clearance at the tumor site by attenuating macrophage infiltration (26). To optimize the therapeutic index of potent oncolytic adenoviruses and sensitize cancer cells to cytotoxic factors, an E1B19K-deleted mutant was therefore constructed with intact E3 and E1B55K genes (Ad5ΔE1B19K).[3]

Here we report on the efficacy and selectivity of novel mutants with and without E1B19K and E3B expression in combination with gemcitabine targeting pancreatic cancers. Treatment with gemcitabine, a cytotoxic nucleotide analogue (2′,2′-difluoro-2′-deoxycytidine; dFdC), results in block of DNA synthesis through chain termination, activation of the DNA damage response, induction of cell death, and inhibition of cell proliferation (27). Our data show that deletion of the E1B19K gene, both in the presence and absence of an intact E3 region, can potently sensitize pancreatic carcinoma cells to gemcitabine-induced death. Combinations of suboptimal doses of oncolytic mutants with gemcitabine resulted in greatly improved cell killing and antitumor efficacy in vivo, with minimal toxicity in normal cells. Although the response was E1A-dependent, neither viral replication nor cell cycle progression was required.

Materials and Methods

Cancer cell lines and adenoviruses

Human pancreatic adenocarcinoma cell lines PT45 and Suit-2 (Cell Services, CRUK) and normal human bronchial epithelial cells (NHBE; Clonetics/Cambrex) were cultured in DMEM supplemented with 10% FCS (Life Technologies) or according to the manufacturer's instructions, respectively. The following viruses and mutants were used: adenovirus type 5 wild-type (Ad5), Ad5ΔE1B19K (E1B19K -deleted Ad5), dl309 (E3B -deleted), dl337 (E1B19K- and E3B-deleted), dl312 (E1A- and E3B-deleted), and AdGFP (cytomegalovirus–green fluorescent protein cassette replacing E1-region). Mutants were constructed using the pAdEasy system (Stratagene) or by recombination of the complete Ad5 genome (28). All viruses used in the study had a viral particle to infectious unit ratio (vp/pfu) of 10–40.

Cell killing assay and synergistic interactions

Cells were infected with viruses and/or treated with gemcitabine (Gemzar; Eli Lilly) 24 h after seeding, assayed 3 or 6 d later using the MTS [3-(4,5-dimethylthiazol-2-yl)-5-(3-carboxymethoxyphenyl)-2-(4-sulfophenyl)-2H-tetrazolium] assay (Promega) to quantify live cells as an indirect measurement of cell death. Dose response curves were generated to calculate the concentration of each agent killing 50% of cells (EC_{50}) using untreated cells or cells treated with one agent only as controls, as previously described (29). Ten-fold dilutions were prepared starting at 1 10^5 particles per cell (ppc) for virus and at 400 μmol/L for gemcitabine. Each data point was generated from triplicate samples and repeated three to five times.

Adenovirus replication assay

Cells were infected with viral mutants at 100 ppc and treated with gemcitabine at 5 nmol/L, 10 nmol/L, or 10 μmol/L, and both simultaneous and sequential additions 24 h apart were evaluated. Cells and media were collected, freeze-thawed, and titered on JH293 cells by the limiting dilution method ($TCID_{50}$; ref. 26). Each assay was repeated two to three times, averaged, and expressed as pfu/cell ± SD. An internal control of known activity was included in each assay.

Quantitative PCR

Cells were infected with viral mutants at 100 ppc and/or treated with gemcitabine at 5 nmol/L, 10 nmol/L, or 10 μmol/L for 3, 24, 48 and 72 h followed by RNA extraction (RNeasy Kit; Qiagen). First-strand cDNA was synthesized from 1 μg total RNA using MMLV-

[3]D. Öberg, et al, unpublished.

Reverse Transcriptase (RT) and random hexamer primers (Taqman; Applied Biosystems). Expression levels of E1A-, penton-, and cellular 18S-mRNAs were determined using the following primers: E1A-forward; 5′-TGCCAAACCTTGTACCGGA-3′, E1A-reverse; 5′-CGTCGTCACTGGGTGGAAA-3′, penton-forward; 5′-GATCGGAAAACCTCTCGAGAAA-3′, penton-reverse; 5′-CGTAGGAGGGAGGAGGACCT-3′, 18S-RNA forward; 5′-CGCCGCTAGAGGTGAAATTC-3′ and reverse; 5′-CATTCTTGGCAAATGCTTTCG-3′. Standard curves were generated using pCR4-TOPO-vectors containing E1A or penton and for 18S cDNA the quantitative PCR (QPCR) reference total RNA (human; Stratagene). QPCR (7500 Real Time PCR System; Applied Biosystems) was done with the Power SYBR Green Master Mix (Applied Biosystems), analyzed by the System SDS software, and expressed as the ratio of E1A or penton cDNA to cellular 18S cDNA (g/g 10^4-10^7) in each sample (n = 2-3). Data are presented from representative studies.

For quantification of viral genome amplification, DNA was isolated from cells treated as described above, and E1A-DNA and hexon-DNA were detected by SYBR Green, with hexon-forward: 5′-GGACAGGCCTACCCTGCTAAC-3′ and reverse: 5′-TGCTGTCAACTGCGGTCTTG-3′. The increase in viral particles over time was expressed as ratio of particles at each time point relative to amount of virus taken up by cells after 3 h (n = 2-3). Data are presented from representative studies.

Immunoblot analysis

Subconfluent cells were infected with viruses in the presence of gemcitabine as described above. Cells were harvested at 24, 48, and 72 h postinfection, lysed in buffer (50 mmol/L Hepes, pH 7.4, 250 mmol/L NaCl, 1 mmol/L EDTA, 1 mmol/L DTT, 1 mmol/L NaF, 1% Triton X-100) containing protease inhibitors. Total protein (10-20 μg) was separated on SDS-polyacrylamide gels under reducing conditions, transferred to polyvinylidene fluoride membranes (Millipore), and detected by the following antisera: rabbit anti-Ad2 E1A at 1:200 (SC-430; Santa Cruz Biotechnology), rabbit antihexon at 1:2000 (AutogenBioclear), and goat antiactin at 1:1000 (SC-1615), rabbit anti-p53 at 1:500 (SC-6243), rabbit anti-cyclin D1 at 1:500 (SC-718), rabbit anti-cyclin E at 1:500 (SC-481), rabbit anti-Cdc25A at 1:2000 (Abcam), mouse anti-p21 waf1 at 1:500 (Calbiochem), mouse anti-caspase-3 at 1:500 (Alexis). Detection was by horseradish peroxidase–conjugated secondary IgG-antibodies (Dako) as appropriate, and chemiluminescence reagent (Amersham/Pharmacia) followed by autoradiography (BioMax film; Kodak).

Flow cytometric analysis

For detection of cell death markers, cells were infected with viruses at 100 ppc for 2 h followed by addition of gemcitabine at 10 nmol/L or 10 μmol/L, harvested 24 to 96 h postinfection and analyzed for caspase-3 activation (Caspase-3 antibody Apoptosis Kit; BD Pharmingen) and Annexin V staining (Alexa Fluor 488 conjugate; Molecular Probes/Invitrogen). Flow cytometry was done on a FACSCalibur instrument (Becton Dickinson), acquiring 10,000 events per sample from duplicate wells using propidium iodide (Sigma-Aldrich) to exclude dead cells and analyzed using CellQuest software. Treated cells were analyzed for changes in mitochondrial membrane potential ($\Delta\psi$), by staining with tetramethylrhodamine ethyl ester perchlorate (Molecular Probes/Invitrogen) at 60 ng/mL in PBS containing 4-6-diamidino-2-phenylindole at 1 μg/mL and analyzed on an LSRI (Becton Dickinson). For cell cycle analysis, cells were treated and harvested as above, washed in PBS, fixed in 70% ethanol for 30 min, treated with 5 μg RNase A (Sigma), and analyzed on a FACSCalibur instrument after addition of 10 μg propidium iodide.

In vivo tumor growth

Tumors were grown in one flank of C57BL athymic (ICRF nu/nu) mice by s.c. implantation of 5 10^6 PT45 cells. Dose responses to viral mutants or gemcitabine were determined by administration of virus intratumorally at 1 10^6 - 10^9 vp/injection three times at 48-h intervals and gemcitabine at 1.0 to 10.0 mg/kg i.p. twice on days 2 to 8 after virus injection. Tumor volumes were estimated twice weekly: volume = (length width^2 π)/6. Treatments were initiated when tumors were 100 ± 20 μL with tumor growth and progression followed until tumors reached 1.44 cm^2 or until symptomatic tumor ulceration occurred (according to UK Home Office Regulations). Treatment groups were balanced by tumor size at the time of treatment initiation (t-test for tumor volumes, **P** > 0.8). Survival analysis expressed as time to progression (tumor volume ≥500 μL) was done according to the method of Kaplan-Meier (log rank test for statistical significance). Tumor growth curves were compared using one-way ANOVA for significance.

Assessment of in vivo gene expression

Following treatments of PT45 xenografts, tumors were harvested 30 to 80 d after the last virus administration and snap-frozen in liquid nitrogen (n = 3 per time point and group). Tumors were processed for immunohistochemistry of E1A and hexon expression (26).

Results

Viral mutant- and gemcitabine-induced, dose-dependent cell death in pancreatic carcinoma cells in culture

Sensitivity to virus- or gemcitabine-induced death was determined in two human pancreatic cell lines, PT45 and Suit2, comparing two E1B19K-deleted mutants, dl337 and Ad5ΔE1B19K, with the respective nondeleted dl309 and Ad5 (Fig. 1A). Both cell lines were relatively insensitive to virus-induced cell death with EC_{50}-values for Ad5 of 532 ± 108 ppc (PT45) and 140 ± 36 ppc (Suit2), for Ad5ΔE1B19K of 994 ± 180 ppc (PT45) and 393 ± 30 ppc (Suit2), and for dl337 and dl309 of 433 ± 118 ppc and 424 ± 110 ppc, respectively, in PT45, and 196 ± 56 ppc and 90 ± 15 ppc, respectively, in Suit2 cells. The nonreplicating mutants dl312 and AdGFP did not induce cell death at doses up to 1 10^5 ppc. Gemcitabine-induced cell death was poor with EC_{50} values of 0.51 ± 0.11 and 0.88 ± 0.23 μmol/L for PT45 and Suit2, respectively, and was significantly less for NHBE cells with 50% of cells killed between 10 and 100 μmol/L.

Low doses of gemcitabine-sensitized PT45 and Suit2 cells to the deletion mutants. To test whether combination treatments could enhance cell death in the relatively resistant cell lines, suboptimal concentrations of gemcitabine were tested at 5 and 10 nmol/L, which kill less than 10% of cells when administered alone. In PT45 cells, both drug concentrations greatly sensitized cells to the ΔE1B19K mutants and significantly less to the nondeleted viruses (Fig. 1B). The same effect was observed in Suit2 cells with greatly and selectively enhanced potency for the ΔE1B19K mutants (Fig. 1C). Similarly, when fixed low doses of 10 or 100 ppc of virus were added, sensitization to gemcitabine with enhanced cell death was observed with both Ad5 and Ad5ΔE1B19K (Supplementary Fig. S1). No enhancement of cell death was detected in response to the combinations in NHBE cells using 5 nmol/L or 10 nmol/L gemcitabine, although a 1,000-fold higher concentration (10 μmol/L) caused significant cell death in combination with both viruses (Fig. 1D).

Gemcitabine inhibits viral replication of all mutants

Surprisingly, in PT45 cells viral replication was completely abrogated in the presence of 10 nmol/L gemcitabine (<1 pfu/cell; Fig. 2A). Suit2 cells supported higher levels of replication

of the virus when used alone but in the presence of gemcitabine, replication was either completely inhibited (Ad5) or detected at very low levels of <4 pfu/cells for the mutants (Fig. 2B). Despite a clear increase in replication over time without drug, both low and high doses of gemcitabine (10 nmol/L and 10 μmol/L) and addition of drug 24 hours prior to or after viral infection, replication was prevented up to 72 hours after gemcitabine treatment. From 96 hours to 144 hours replication was detectable although still significantly attenuated (Supplementary Fig. S2C). Attenuation was also observed to varying degrees in other cell lines and with other viral mutants exemplified by the ovarian SKOV3 cells (Supplementary Fig. S2B). The inhibition was not due to loss in cell viability; after 72 hours more than 85% of cells were viable with 10 nmol/L gemcitabine. However, cell death could have contributed at the higher dose level (10 μmol/L) resulting in only 65% and 40% viable PT45 and Suit2 cells, respectively, after 72 hours. The normal NHBE cells supported replication of all mutants, but in combination with gemcitabine viral replication was potently attenuated at all tested concentrations (Fig. 2C). To verify these novel observations, PT45 cells were analyzed for amplification of viral genomes by QPCR (Fig. 2D). In Ad5ΔE1B19K-infected cells, a >7-fold increase in viral DNA was determined 24 hours after infection when compared with internalized virus 3 hours after infection, whereas cells treated with 10 nmol/L gemcitabine did not amplify viral DNA above the uptake level. After 48 hours, a further increase in amplification was observed in cells infected with virus alone whereas in the presence of gemcitabine no significant increase was detected (Fig. 2D). Identical results were observed in the Suit2 cells and in wild-type virus–treated cells (Supplementary Fig. S2A and data not shown).

Gemcitabine decreases viral gene expression

Despite attenuation of viral replication in the presence of gemcitabine, E1A-proteins were highly expressed over time with all mutants although at slightly lower levels than with virus alone (Fig. 3A and B). Quantitative analysis of E1A mRNA levels showed a clear attenuation in the presence of 10 nmol/L gemcitabine compared with cells infected with virus alone (Fig. 3C). Consistent with the replication data, hexon expression was suppressed in the presence of gemcitabine at 48 hours with all mutants, but expressed after 72 hours (Fig. 3B). A parallel delay in expression of penton transcripts was observed with low levels at 48 hours and slightly increased after 72 hours (Fig. 3D). These data show that sufficient quantities of E1A were present to enable sensitization to the cytotoxic effects of gemcitabine in the absence of viral replication. Interestingly, expression of E1A was also sustained in the NHBE cells up to 72 hours after gemcitabine addition followed by cell detachment and death (Fig. 3B, lower panel). This was in contrast to cells infected with virus alone that were more rapidly detached as a result of potent viral replication (Fig. 2C).

Low concentration of gemcitabine delay S-phase progression in PT45 cells

Cell cycle analysis of PT45 cells treated with 10 nmol/L gemcitabine showed arrest of the G_1/S-phase up to 48 hours after initial addition of drug followed by gradual escape with increased fractions in G_2 and sub-G_1 (Fig. 4A and B). With 10 μmol/L gemcitabine, a high proportion of cells were dying already during early (24-48 hours) time points resulting in few attached cells and a higher proportion of cells in the sub-G_1 fraction in the remaining cells (Fig. 4B). No virally induced effects on cell cycle progression could be detected under these nonsynchronized conditions (Fig. 4A). When viruses and drug were combined, the sub-G_1 population increased after 72 to 96 hours with all mutants, exemplified with the data for Ad5ΔE1B19K (Fig. 4A and B).

Gemcitabine prevents virus induction of S-phase cyclins

As expected from the cell cycle data, p21 was elevated in response to 10 nmol/L gemcitabine and remained high in the presence of all mutants (Fig. 4C). Basal cyclin D

levels were maintained after virus infection but attenuated after the addition of gemcitabine. All viral mutants induced cyclin E and cdc25A whereas gemcitabine inhibited both virus-induced and basal expression. These results show that viral E1A expression is not sufficient to overcome the gemcitabine-induced arrest in response to DNA damage causing attenuation of replication. The mutant version of p53 present in PT45 cells was constitutively expressed at high levels with no changes corresponding to the drug-induced increase in p21. Cells treated with 10 μmol/L gemcitabine did not show an increase in p21 levels at 24 to 72 hours as expected from the higher levels of cell death and lack of a clear cell cycle arrest under the test conditions (Figs. 4B, Supplementary Fig. S3). To verify the G_1-early S-phase arrest as a cause for the attenuated viral replication aphidocholine, a potent blocker of early S-phase, was combined with the viral mutants (Fig. 4D, right). As expected, viral replication was decreased in the presence of this potent DNA-polymerase inhibitor even at low concentrations (Fig. 4D, left).

Apoptosis-like cell death is increased in response to combination treatments of ΔE1B19K mutants and gemcitabine

Excluding viral replication as a cause of the enhancement, the mode of cell death in response to viral gene expression and gemcitabine was explored. We hypothesized that ΔE1B19K mutants could enhance gemcitabine-induced apoptotic death and determined exposure of phosphatidylserine and uptake of propidium iodide. Total apoptotic death (annexin- and propidium iodide–positive) was increased with all viruses in combination with gemcitabine after 48 to 96 hours (Fig. 5A and data not shown). Significant enhancement was observed in cells treated with mutant viruses but not in Ad5-infected cells. The increase in apoptotic death was greatest in combination with the ΔE1B19K mutants, with a >5% increase above what would be expected for simply additive levels. Similarly, activation of caspase-3 showed a clear synergistic enhancement with all viruses in combination with gemcitabine, with the greatest effects in cells infected with the ΔE1B19K mutants (Fig. 5B and Supplementary Fig. S4). Cleavage of procaspase to active caspase-3 was verified by immunoblotting under the same treatment conditions (Fig. 5B, insert). To investigate activation of apoptotic mechanisms upstream of caspase-3, changes in mitochondrial membrane potential ($\Delta\psi$) were determined by tetramethylrhodamine ethyl ester staining from 24 to 96 hours (Figs. 5C and Supplementary Fig. S5). No change in membrane potential was observed with viral mutants alone whereas gemcitabine treatment resulted in significant loss of staining. The greatest decrease in membrane potential was in combination with 10 μmol/L gemcitabine and both wild-type and mutant viruses 48 to 96 hours posttreatment (Fig. 5C, left panel). Combinations with the lower dose of 10 nmol/L resulted in a greater loss of potential with the Ad5ΔE1B19K up to 96 hours after treatment (Fig. 5C, right panel, and Supplementary 5S). Addition of the pan-caspase inhibitor zVAD-fmk completely blocked the enhancement of cell death in response to combination treatment with no significant effect on virus-induced death alone (Fig. 5D, left panel). Gemcitabine-induced cell death was attenuated in a dose-dependent manner (Fig. 5D, right panel). Taken together these results show that both E1B19K-deleted and wild-type viruses potentiate gemcitabine-induced apoptotic cell death through induction of mitochondrial membrane dysfunction followed by caspase-3 activation. The induction was more potent with both ΔE1B19K mutants.

Combination of low doses of gemcitabine and Ad5ΔE1B19K greatly inhibit tumor growth of PT45 xenografts in vivo

The potency of the combination treatments was evaluated in an in vivo PT45 xenograft model with s.c. tumors treated with suboptimal doses of Ad5ΔE1B19K, Ad5, and nonreplicating control virus or with gemcitabine (Fig. 6A and B). In animals treated with the lowest dose of virus at 1 10^6 vp, no significant tumor regression or increase in survival was

observed; median survival was 12.5 days for mock versus 35 days for Ad5ΔE1B19K. In combination with 2.5 mg/kg of gemcitabine, time to progression was prolonged to 117 days compared with 35 days and 52 days with each agent alone. Because the higher dose of virus ($1\ 10^7$ vp) resulted in >80% of animals not having progressed at the end of the study (130 days), no improvements in combination with either drug concentration could be determined. However, when the lower virus dose was combined with the higher gemcitabine dose (5 mg/kg) both tumor growth inhibition and prolonged time to progression were observed; median survival was >130 days compared with 35 days and 63 days for each single treatment. In fact, this combination resulted in the same efficacy as the higher dose of virus and was superior to the highest dose of drug. Similar efficacy was determined in combination with Ad5 (Table 1 and data not shown).

In a separate study, Ad5 and Ad5ΔE1B19K were combined with lower doses of gemcitabine at 1 and 2.5 mg/kg, resulting in significant improvements only in combination with the higher dose of drug (Table 1). The corresponding tumor samples stained positive for hexon expression up to 60 days after viral administration both with and without gemcitabine (Fig. 6C). E1A-positive cells could be detected in xenografts treated with the combinations up to 76 days after treatment. E1A-deleted and green fluorescent protein – expressing, E1-deleted, nonreplicating mutants had no efficacy in this model and in combination with gemcitabine did not further inhibit tumor growth nor improve time to progression compared with drug treatment alone (Table 1).

Discussion

Our results show that antitumor efficacy was greatly improved when E1B19K-deleted mutants were combined with subtherapeutic concentrations of the cytotoxic drug gemcitabine. In addition, the sensitization was specific for cancer cells and did not occur in normal cultured cells. Although we and others previously proposed incorporation of the E1B19K deletion in already potent replication-selective oncolytic mutants, this gene deletion had not been studied on its own (16–18, 20, 22, 25). Mutants with additional deletions in death-related genes such as ADP, E1B55K, or E3B were reported to have higher potency and improved spread in cancer cells. During viral infection the E1B55K and E3B genes protect against p53- and death receptor–induced apoptosis, respectively. The Ad5ΔE1B19K mutant used in this study was engineered to lack only the E1B19K antiapoptotic gene and was compared with mutants with E3B deletions with and without E1B19K. Our goal was to establish the role of a single E1B19K deletion in the background of an intact Ad5 backbone prior to construction of combination mutants for oncolytic therapy. For the first time, we showed that enhancement of cell death could be achieved with both the single deletion (Ad5ΔE1B19K) and the additional E3B deletion (dl337) in combination with suboptimal doses of gemcitabine. Although wild-type viruses with intact E1B19K could sensitize cells, the effect was significantly less than with the corresponding mutants. No sensitization was detected in normal cells, which is likely due to the much higher threshold of gemcitabine toxicity (EC_{50} >10 μmol/L) and perhaps a more efficient antiviral response. These findings suggest that pancreatic adenocarcinomas could be efficiently targeted by less toxic doses than currently practiced in the clinic if combined with oncolytic mutants lacking the antiapoptotic E1B19K gene.

Interestingly, the potent increase in cell death in response to combination treatment was not dependent on viral replication. In fact, replication was prevented in response to all tested concentrations of gemcitabine, a finding not previously reported. Our data showed a nearly complete inhibition up to 72 hours after treatment with detectable levels first at later time points. Other investigators using the modified oncolytic mutant Ad5/3-Δ24 combined with gemcitabine in the ovarian carcinoma cell line SKOV-3 reported a reduction in the initial

replication rate whereas total viral yield was unaffected after 96 hours at μmol/L concentrations (30). Although we observed a greater attenuation of replication with Ad5 and Ad5μCR2 in SKOV-3 cells combined with 10 nmol/L and 10 μmol/L gemcitabine than reported by Raki et al (30), a similar trend was seen with replication resuming over time paralleling the escape from gemcitabine-induced cell cycle arrest. Gemcitabine-induced attenuation of replication was also reported for replication-selective herpes mutants targeting the pancreatic Capan1, Paca2, and SW1990 human carcinomas (31), whereas in other studies both gemcitabine and fluorouracil were found to stimulate herpes simplex virus replication in pancreatic Hs700T cells (32). Recently, Toth et al. reported that a related cidofovir derivative, CMX001, could potently inhibit adenoviral replication in immunosuppressed hamsters (33). In addition, the cytotoxic drug arabinofuranosylcytosine (Ara-C), a structural and functional analogue to gemcitabine, is an established potent inhibitor of viral replication. Here, we showed gemcitabine-induced G_1/S-cell cycle block as a cause for the attenuated replication further verified by the S-phase blocker aphidocholine. Arrest of cell cycle progression is likely dependent on the sensitivity to cytotoxic drugs and viral mutants of each cell line and clearly determines whether viral replication will proceed. The role of cycle arrest was not explored in other studies (30–32). Gemcitabine was previously shown to induce a dose-dependent delay of cell cycle progression in G_1/S-phase followed by impaired DNA synthesis with cytostatic or cytotoxic effects on viability, dependent on cell line (34). We found that lower doses of gemcitabine arrested cells in G_1/S up to 48 hours and higher doses were immediately cytotoxic. The arrest indicates activation of the chk1 restriction point in response to DNA -breaks resulting in phosphorylation and deactivation of cdc25A. Adenovirus replication is entirely dependent on cellular DNA synthesis involving multiple mechanisms to ensure induction of S-phase in infected cells. One of these mechanisms, induction of cdc25A/cyclin E/cdk2 expression and activation by the viral E1A gene, was reported as an absolute requirement for replication in certain cell types (35, 36). In our study gemcitabine-induced arrest decreased cyclin E and cdc25A levels, a decrease that could not be overcome by viral E1A expression. Consequently, cellular DNA synthesis did not proceed to support viral propagation.

A major finding in our report was that cell death in response to virus and gemcitabine occurred through enhancement of drug-induced apoptosis with synergistic increases in combination with the E1B19K-deleted mutants. Differently from cytotoxic drugs such as gemcitabine that induce death through classical apoptosis including DNA damage, mitochondrial depolarization, caspase activation, and nuclear fragmentation, adenoviruses activate cell death though nonapoptotic pathways (37, 38). Although drug-induced caspase-3 activation and loss of mitochondrial potential was enhanced in combination with all viruses, the greatest increase was with the ΔE1B19K mutants. This difference in enhancement was more obvious in the later apoptotic events of membrane fragmentation and exposure of phosphatidylserine where the ΔE1B19K mutants were far more potent than the corresponding wild-type viruses. In agreement with previous studies, no activation of apoptosis was detected with any mutant when given alone although we clearly proved a synergistic increase at several steps in the gemcitabine-induced apoptotic response when combined. A probable cause for the increased apoptotic effects in combination with ΔE1B19K mutants is the proapoptotic function of the E1A products. E1A has been shown to suppress anchorage-independent tumor cell growth, inhibit oncogenes, and directly act on death signaling pathways and to increase cell sensitivity to cytotoxic drugs such as paclitaxel, adriamycin, etoposide, and gemcitabine in carcinoma cells (19, 39–43). In the previous studies an E1A-expressing vector was used and consequently no other viral genes were present to inhibit the apoptotic responses such as the E1B55K, E1B19K, or E3 genes. Similar findings were also reported using replicating viruses with specific gene deletions, suggesting that apoptotic functions of the E1A gene could be blocked by expression of the E1B and E3 genes (44, 45). We speculate that by deleting E1B19K the proapoptotic

functions of E1A were not counteracted, further pushing the balance towards apoptosis in the presence of DNA-damaging drugs.

The in vivo studies reported here show the feasibility of combination treatments of oncolytic mutants and DNA-damaging drugs. Both tumor growth inhibition and time to progression were significantly improved when combining doses of virus and gemcitabine that when given alone did not have antitumor efficacy. Despite attenuation of viral replication in cultured cells, we showed potent early and late viral gene expression in vivo up to 30 to 76 days after initial treatment, although whether replication occurred could not be evaluated in these studies. The data show that viral gene expression was sustained for a long period of time in vivo and indicate long-lasting effects on drug sensitization. In our study, gemcitabine and viruses were delivered i.p. and intratumorally, respectively, and most likely drug doses at the tumor site were lower than anticipated perhaps allowing viral replication to proceed. Additional studies would be required to determine the bioavailability, distribution, and half-life of gemcitabine in these models. Both virus and drug were administered at several different time points possibly facilitating viral spread by drug-induced tissue elimination and suppression of the innate immune response preventing virus elimination. To fully understand the underlying mechanisms of these observations necessitates further investigations. Nevertheless, the clinical implications of possible dose reductions hold promise for improved efficacy and less treatment-associated toxicities in future applications. Interestingly, viral replication was also attenuated in the normal NHBE cells indicating improved safety in the clinical setting. In addition, our previous work suggests that normal cells infected with ΔE1B19K mutants in vivo would be eliminated through tumor necrosis factor–induced apoptosis (16), thus preventing viral spread in normal tissue and further improving the therapeutic index.

Overall our findings show that incorporation of the E1B19K deletion in replication-selective adenoviruses significantly enhanced efficacy of combination therapies with DNA-damaging cytotoxic chemotherapy. The sensitization to gemcitabine-induced apoptosis was retained even in the presence of intact E1B55K and E3B genes. These findings will aid in the selection of future oncolytic mutants that are likely to incorporate both E1B55K and E3B genes based on previous poor efficacy in vivo when these genes were deleted (5–9, 26). Further studies to investigate whether the enhancement is caused by E1A proapoptotic functions, DNA-damage response, or specific gene alterations and verification in drug- and viral replication –resistant tumor cells will be essential for understanding virus-drug-host interactions.

Translational Relevance

Pancreatic adenocarcinoma is an aggressive malignancy, highly resistant to current chemotherapeutic modalities, which is among the leading causes of cancer-related deaths globally because it presents late at an advanced stage. The current standard of care is gemcitabine but although this produces extension of survival it is rarely curative. Here we show that oncolytic mutants with deletion of the antiapoptotic *E1B19K* gene can significantly improve the antitumor efficacy of gemcitabine through the enhancement of cell death through apoptosis.

These findings are important for the future design of combination therapies and particularly the potential of oncolytic mutants to target gemcitabine-insensitive cancers.

Acknowledgments

We thank Gary Martin and colleagues at Clare Hall (CRUK) for excellent experimental assistance; Jennelle Francis andVipul Bhakta (Molecular Oncology Unit) for virus production and QPCR expertise; and Yaohe Wang, Siew Chiat Cheong, and Gioia Cherubini for critical reading of the manuscript and insightful discussions.

Grant support: Cancer Research UK Programme Grants C355/A6251 C355/6252 and C355/A6253; Digestive Cancer Campaign Programme Grant; Barts and The London Charity Flavell Programme inViral GeneTherapy.

References

1. Jemal A, Murray T, Ward E, et al. Cancer statistics, 2005. CA Cancer J Clin. 2005; 55:10–30. [PubMed: 15661684]
2. Oettle H, Post S, Neuhaus P, et al. Adjuvant chemotherapy with gemcitabine vs observation in patients undergoing curative-intent resection of pancreatic cancer: a randomized controlled trial. JAMA. 2007; 297:267–77. [PubMed: 17227978]
3. Kasuya H, Takeda S, Nomoto S, Nakao A. The potential of oncolytic virus therapy for pancreatic cancer. Cancer GeneTher. 2005; 12:725–36.
4. Harada JN, Berk AJ. p53-Independent and -dependent requirements for E1B–55K in adenovirus type 5 replication. J Virol. 1999; 73:5333–44. [PubMed: 10364280]
5. O'Shea CC, Johnson L, Bagus B, et al. Late viral RNA export, rather than p53 inactivation, determines ONYX-015 tumor selectivity. Cancer Cell. 2004; 6:611–23. [PubMed: 15607965]
6. Khuri FR, Nemunaitis J, Ganly I, et al. a controlled trial of intratumoral ONYX-015, a selectively-replicating adenovirus, in combination with cisplatin and 5-fluorouracil in patients with recurrent head and neck cancer. Nat Med. 2000; 6:879–85. [PubMed: 10932224]
7. Xia ZJ, Chang JH, Zhang L, et al. [Phase III randomized clinical trial of intratumoral injection of E1B gene-deleted adenovirus (H101) combined with cisplatin-based chemotherapy in treating squamous cell cancer of head and neck or esophagus.]. Ai Zheng. 2004; 23:1666–70. [PubMed: 15601557]
8. Mulvihill S, Warren R, Venook A, et al. Safety and feasibility of injection with an E1B-55 kDa gene-deleted, replication-selective adenovirus (ONYX-015) into primary carcinomas of the pancreas: a phase I trial. Gene Ther. 2001; 8:308–15. [PubMed: 11313805]
9. Hecht JR, Bedford R, Abbruzzese JL, et al. A phase I/II trial of intratumoral endoscopic ultrasound injection of ONYX-015 with intravenous gemcitabine in unresectable pancreatic carcinoma. Clin Cancer Res. 2003; 9:555–61. [PubMed: 12576418]
10. Heise C, Hermiston T, Johnson L, et al. An adenovirus E1A mutant that demonstrates potent and selective systemic anti-tumoral efficacy. Nat Med. 2000; 6:1134–9. [PubMed: 11017145]
11. Stolarek R, Gomez-Manzano C, Jiang H, Suttle G, Lemoine MG, Fueyo J. Robust infectivity and replication of Δ-24 adenovirus induce cell death in human medulloblastoma. Cancer Gene Ther. 2004; 11:713–20. [PubMed: 15332115]
12. Small EJ, Carducci MA, Burke JM, et al. A phase I trial of intravenous CG7870, a replication-selective, prostate-specific antigen-targeted oncolytic adenovirus, for the treatment of hormone-refractory, metastatic prostate cancer. Mol Ther. 2006; 14:107–17. [PubMed: 16690359]
13. DeWeese TL, van der Poel H, Li S, et al. A phase I trial of CV706, a replication-competent, PSA selective oncolytic adenovirus, for the treatment of locally recurrent prostate cancer following radiation therapy. Cancer Res. 2001; 61:7464–72. [PubMed: 11606381]
14. Johnson L, Shen A, Boyle L, et al. Selectively replicating adenoviruses targeting deregulated E2F activity are potent, systemic antitumor agents. Cancer Cell. 2002; 1:325–37. [PubMed: 12086848]
15. Schepelmann S, Hallenbeck P, Ogilvie LM, et al. Systemic gene-directed enzyme prodrug therapy of hepatocellular carcinoma using a targeted adenovirus armed with carboxypeptidase G2. Cancer Res. 2005; 65:5003–8. [PubMed: 15958540]
16. Liu TC, Hallden G, Wang Y, et al. An E1B-19 kDa gene deletion mutant adenovirus demonstrates tumor necrosis factor-enhanced cancer selectivity and enhanced oncolytic potency. Mol Ther. 2004; 9:786–803. [PubMed: 15194046]

17. Sauthoff H, Heitner S, Rom WN, Hay JG. Deletion of the adenoviral E1b-19kD gene enhances tumor cell killing of a replicating adenoviral vector. Hum Gene Ther. 2000; 11:379–88. [PubMed: 10697113]
18. Yoon AR, Kim JH, Lee YS, et al. Markedly enhanced cytolysis by E1B–19kD-deleted oncolytic adenovirus in combination with cisplatin. Hum Gene Ther. 2006; 17:379–90. [PubMed: 16610926]
19. White E. Regulation of the cell cycle and apoptosis by the oncogenes of adenovirus. Oncogene. 2001; 20:7836–46. [PubMed: 11753666]
20. Subramanian T, Vijayalingam S, Chinnadurai G. Genetic identification of adenovirus type 5 genes that influence viral spread. J Virol. 2006; 80:2000–12. [PubMed: 16439556]
21. Putzer BM, Stiewe T, Parssanedjad K, Rega S, Esche H. E1A is sufficient by itself to induce apoptosis independent of p53 and other adenoviral gene products. Cell Death Differ. 2000; 7:177–88. [PubMed: 10713732]
22. Lomonosova E, Subramanian T, Chinnadurai G. Mitochondrial localization of p53 during adenovirus infection and regulation of its activity by E1B-19K. Oncogene. 2005; 24:6796–808. [PubMed: 16007153]
23. Cross JR, Postigo A, Blight K, Downward J. Viral pro-survival proteins block separate stages in Bax activation but changes in mitochondrial ultrastructure still occur. Cell Death Differ. 2008; 15:997–1008. [PubMed: 18274554]
24. Liu TC, Wang Y, Hallden G, et al. Functional interactions of antiapoptotic proteins and tumor necrosis factor in the context of a replication-competent adenovirus. GeneTher. 2005; 12:1333–46.
25. Harrison D, Sauthoff H, Heitner S, Jagirdar J, Rom WN, Hay JG. Wild-type adenovirus decreases tumor xenograft growth, but despite viral persistence complete tumor responses are rarely achieved - deletion of the viral E1b-19-kD gene increases the viral oncolytic effect. Hum GeneTher. 2001; 12:1323–32.
26. Wang Y, Hallden G, Hill R, et al. E3 gene manipulations affect oncolytic adenovirus activity in immunocompetent tumor models. Nat Biotechnol. 2003; 21:1328–35. [PubMed: 14555956]
27. Heinemann V, Schulz L, Issels RD, Plunkett W. Gemcitabine: a modulator of intracellular nucleotide and deoxynucleotide metabolism. Semin Oncol. 1995; 22:11–8. [PubMed: 7481839]
28. Chartier C, Degryse E, Gantzer M, Dieterle A, Pavirani A, Mehtali M. Efficient generation of recombinant adenovirus vectors by homologous recombination in Escherichia coli. J Virol. 1996; 70:4805–10. [PubMed: 8676512]
29. Cheong SC, Wang Y, Meng JH, et al. E1A-expressing adenoviral E3B mutants act synergistically with chemotherapeutics in immunocompetent tumor models. Cancer GeneTher. 2008; 15:40–50.
30. Raki M, Kanerva A, Ristimaki A, et al. Combination of gemcitabine and Ad5/3-Δ24, a tropism modified conditionally replicating adenovirus, for the treatment of ovarian cancer. GeneTher. 2005; 12:1198–205.
31. Watanabe I, Kasuya H, Nomura N, et al. Effects of tumor selective replication-competent herpes viruses in combination with gemcitabine on pancreatic cancer. Cancer Chemother Pharmacol. 2008; 61:875–82. [PubMed: 17726607]
32. Eisenberg DP, Adusumilli PS, Hendershott KJ, et al. 5-fluorouracil and gemcitabine potentiate the efficacy of oncolytic herpes viral gene therapy in the treatment of pancreatic cancer. J Gastrointest Surg. 2005; 9:1068–77. discussion 77-9. [PubMed: 16269377]
33. Toth K, Spencer JF, Dhar D, et al. Hexadecyloxy-propyl-cidofovir, CMX001, prevents adenovirus-induced mortality in a permissive, immunosuppressed animal model. Proc Natl Acad Sci U S A. 2008; 105:7293–7. [PubMed: 18490659]
34. Cappella P, Tomasoni D, Faretta M, et al. Cell cycle effects of gemcitabine. Int J Cancer. 2001; 93:401–8. [PubMed: 11433406]
35. Spitkovsky D, Jansen-Durr P, Karsenti E, Hoffman I. S-phase induction by adenovirus E1A requires activation of cdc25a tyrosine phosphatase. Oncogene. 1996; 12:2549–54. [PubMed: 8700513]
36. Bonapace IM, Latella L, Papait R, et al. Np95 is regulated by E1A during mitotic reactivation of terminally differentiated cells and is essential for S phase entry. J Cell Biol. 2002; 157:909–14. [PubMed: 12058012]

37. Abou, El; Hassan, MA.; van der Meulen-Muileman, I.; Abbas, S.; Kruyt, FA. Conditionally replicating adenoviruses kill tumor cells via a basic apoptotic machinery-independent mechanism that resembles necrosis-like programmed cell death. J Virol. 2004; 78:12243–51. [PubMed: 15507611]

38. Baird SK, Aerts JL, Eddaoudi A, Lockley M, Lemoine NR, McNeish IA. Oncolytic adenoviral mutants induce a novel mode of programmed cell death in ovarian cancer. Oncogene. 2008; 27:3081–90. [PubMed: 18071311]

39. Chattopadhyay D, Ghosh MK, Mal A, Harter ML. Inactivation of p21by E1A leads to the induction of apoptosis in DNA-damaged cells. J Virol. 2001; 75:9844–56. [PubMed: 11559818]

40. Yu D, Wolf JK, Scanlon M, Price JE, Hung MC. Enhanced c-erbB-2/neu expression in human ovarian cancer cells correlates with more severe malignancy that can be suppressed by E1A. Cancer Res. 1993; 53:891–8. [PubMed: 8094034]

41. Ueno NT, Bartholomeusz C, Herrmann JL, et al. E1A-mediated paclitaxel sensitization in HER-2/neuoverexpressing ovarian cancer SKOV3.ip1 through apoptosis involving the caspase-3 pathway. Clin Cancer Res. 2000; 6:250–9. [PubMed: 10656456]

42. Zhou Z, Jia SF, Hung MC, Kleinerman ES. E1A sensitizes HER2/neu-overexpressing Ewing's sarcoma cells to topoisomerase II-targeting anticancer drugs. Cancer Res. 2001; 61:3394–8. [PubMed: 11309298]

43. Lee WP, Tai DI, Tsai SL, et al. Adenovirus type 5 E1A sensitizes hepatocellular carcinoma cells to gemcitabine. Cancer Res. 2003; 63:6229–36. [PubMed: 14559808]

44. Rao XM, Tseng MT, Zheng X, et al. E1A-induced apoptosis does not prevent replication of adenoviruses with deletion of E1b in majority of infected cancer cells. Cancer GeneTher. 2004; 11:585–93.

45. Hu B, Zhu H, Qiu S, et al. Enhanced TRAIL sensitivity by E1A expression in human cancer and normal cell lines: inhibition by adenovirus E1B19K and E3 proteins. Biochem Biophys Res Commun. 2004; 325:1153–62. [PubMed: 15555548]

Europe PMC Funders Author Manuscripts

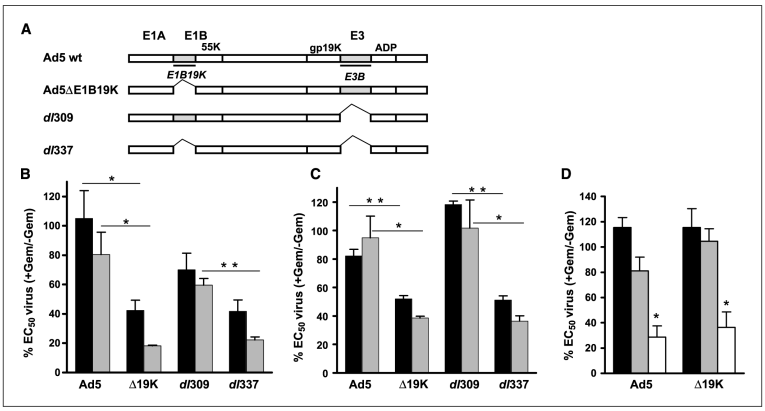

Fig. 1.

Low doses of gemcitabine sensitize pancreatic cancer but not normal cells to *E1B19K*-deleted mutants. *A*, viruses used in the study with the respective deletions indicated. PT45 (*B*) and Suit2 (*C*) cells were infected with viruses and treated with 5 nmol/L (*black*) or 10 nmol/L (*grey*) gemcitabine. *D*, normal NHBE cells infected with mutants and treated with 5 nmol/L (*black*), 10 nmol/L (*grey*) or10 μmol/L (*white*) gemcitabine. Cells were analyzed for viability with the MTS assay 3 d after treatment; EC_{50} values were calculated and presented as percentages of virus-treated compared with control cells, as described in Materials and Methods. Data are the averages of three to four experiments ± SE; $*P < 0.05$ and $**P < 0.01$for *B* and *C*, and *D* is the average of one representative study in triplicate ± SE with $*P < 0.05$ compared with virus-treated cells.

Europe PMC Funders Author Manuscripts

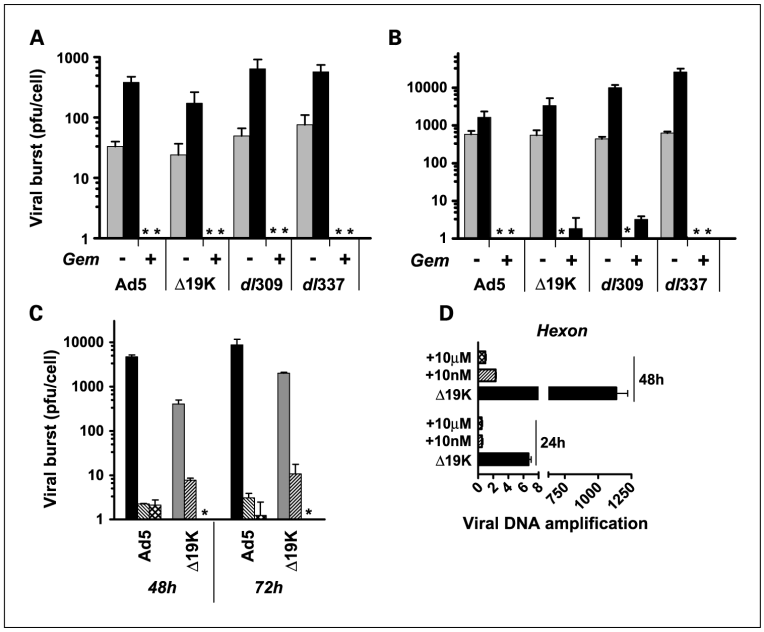

Fig. 2.

Gemcitabine prevents viral replication in PT45 and Suit2 pancreatic cell lines and in normal cells. *A*, replication in PT45 and (*B*) Suit 2 cells was analyzed after 48 h (*grey*) and 72 h (*black*) of treatment with 10 nmol/L gemcitabine, and (*C*) NHBE cells after 48 h and 72 h of treatment with viruses alone (*black or grey*) and in combination with gemcitabine at 10 nmol/L (*striped*) and 10 μmol/L (*crossed*).Virus and drug were added simultaneously and both cells and media were analyzed by$TCID_{50}$ assays. The data are from a representative of three experiments. The * indicates that replication levels were below the detection limit of the assay, < 1pfu/cell. *D*, QPCR of viral DNA in PT45 cells 24 and 48 h after infection.Viral DNA copies were determined after treatment with 10 nmol/L (*striped*) and 10 μmol/L (*crossed*) gemcitabine or with the Ad5ΔE1B19K virus alone (*black*). Gene amplification was normalized to input virus (3 h after infection; $n = 3$).

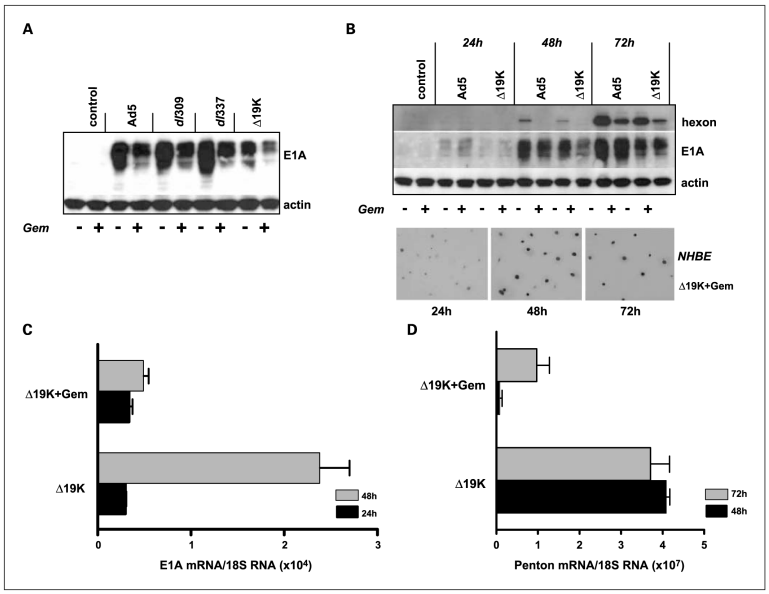

Fig. 3.

Early and late viral genes are expressed in PT45 cells infected with viral mutants in the presence of gemcitabine. A, immunoblot of cells infected with Ad5, Ad5ΔE1B19K, *dl*309, or *dl*337 and treated with 10 nmol/L gemcitabine. Cell extracts were prepared 48 h after infection and 20 μg of protein loaded in each lane for detection of E1A expression. *B*, cells infected with Ad5wt and Ad5ΔE1B19K harvested 24 to 72 h after infection and analyzed for E1A and hexon expression (*upper panel*). Lower panel, light microscopy of NHBE cells grown on glass slides, infected with AdΔ19K in the presence of 10 nmol/L gemcitabine, stained for E1A expression at 24 to 72 h, magnification 200. *C*, quantitative reverse transcription-PCR of E1A and (*D*) penton mRNA levels in response to gemcitabine 24, 48, and 72 h after treatment. Standard curves were prepared for each gene and results were normalized to 18S RNA in every sample, as described in Materials and Methods. Data are representative of two to three experiments.

Europe PMC Funders Author Manuscripts

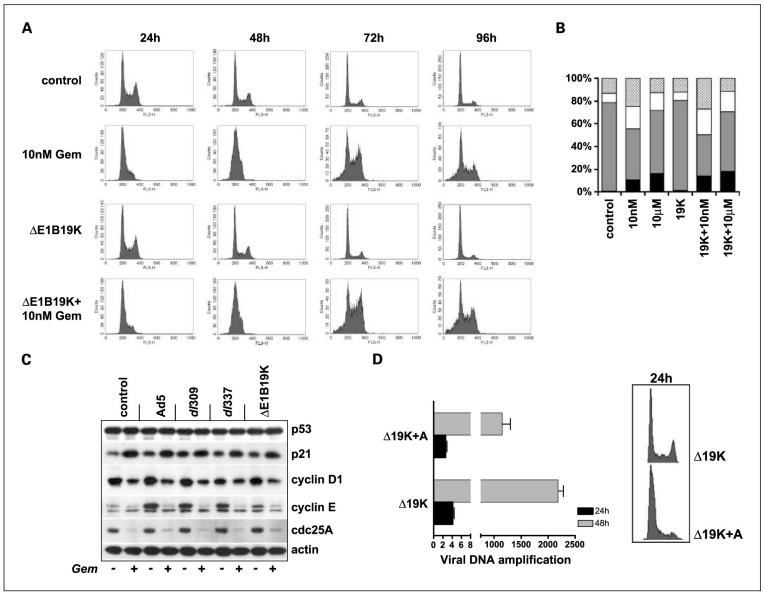

Fig. 4.

Cell cycle analysis of PT45 cells in the presence of viral mutants and gemcitabine. *A*, flow cytometric analysis of cells treated with gemcitabine at 10 nmol/L, the Ad5ΔE1B19K mutant alone or in combination. Cells were fixed and stained with propidium iodide 24, 48, 72, and 96 h after treatment. *B*, histograms illustrating the cell cycle-phase distribution in percentages in response to combination treatments with 10 nmol/L or 10 μmol/L gemcitabine and the ΔE1B19K mutant 96 h after treatment; sub-G_1 (*black*), G_1 (*grey*), S (*white*), and G_2/M (*top light grey*). *C*, immunoblot of changes in expression levels of cell cycle related proteins in response to mutants and gemcitabine (10 nmol/L) combinations. Cells were harvested 72 h after treatment. *D*, cells were serum-starved and treated with aphidocholine (5 μg/mL) for 24 and 48 h followed by viral DNA (hexon) amplification (*left panel*); right, the corresponding cell cycle diagram 24 h after addition of aphidocholine. Gene amplification was normalized to input virus (3 h after infection); data are representative of three studies.

Europe PMC Funders Author Manuscripts

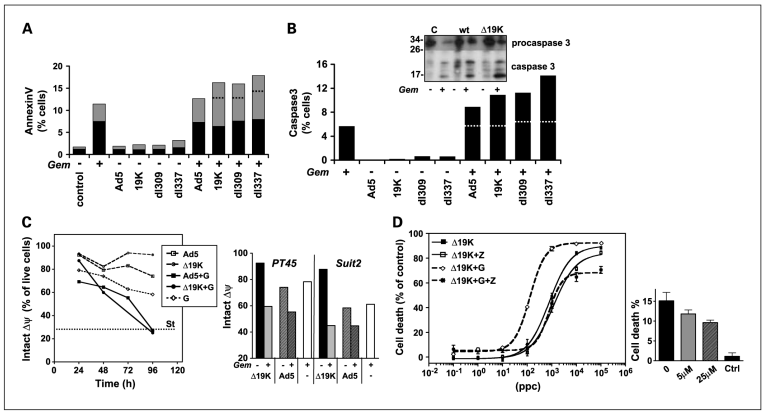

Fig. 5.

Combination treatment enhances gemcitabine-induced apoptotic cell death in PT45 cells. *A*, PT45 cells were treated with 100 ppc of each viral mutant with and without 10 nmol/L gemcitabine for 72 h and analyzed for cell death using an Annexin Vantibody and propidium iodide. Lower black bars, annexin positive only; upper grey bars, both annexin- and propidium iodide–positive cells; dashed lines, predicted additive value of total apoptotic cells (annexin positive ± propidium iodide staining). *B*, cells were treated as in *A* and analyzed by a specific antibody for active caspase-3 by flow cytometry, 72 h after treatment initiation. Dashed lines, predicted additive values of combination treatments. Insert, immunoblot of inactive procaspase-3 (34 kD) and the active cleaved caspase-3 subunits (17 and 20 kD) at the same time point. *C*, changes in mitochondrial membrane potential ($\Delta\psi$) determined by tetramethylrhodamine ethyl ester perchlorate (TMRE) staining and cytometry analysis, expressed as % of live cells with unchanged $\Delta\psi$ (TMRE-positive only). Cells were treated with 10 μmol/L gemcitabine alone or in combination with 100 ppc of each viral mutant. Staurosporin (St)-treated cells (3 μmol/L) were included as a reference for mitochondrial dysfunction (*left panel*). Right panel, $\Delta\psi$ in response to combinations of mutant or Ad5 with gemcitabine (10 nmol/L) at 96 h in PT45 and Suit2 cells. Representative data from four to six studies. *D*, dose response to Ad5ΔE1B19K alone and in combination with 10 nmol/L gemcitabine (G) with and without the pan-caspase inhibitor zVAD-fmk (Z) at 25 μmol/L. Cell death was determined by MTS assay (*left panel*). Right, inhibition of cell death by zVAD-fmk (Z) at 5 and 25 μmol/L in gemcitabine-treated (20 nmol/L) and untreated control cells (Ctrl; 25 μmol/L Z). Data are representative of three experiments with triplicate samples for each study in *A*, *B*, and *D*.

Europe PMC Funders Author Manuscripts

Europe PMC Funders Author Manuscripts

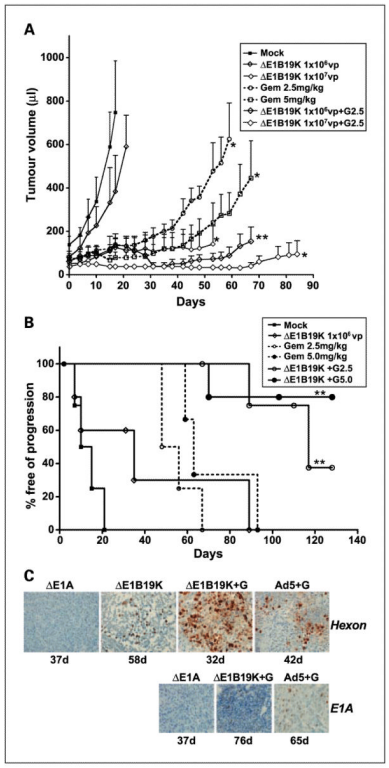

Fig. 6.

Combinations of low doses of the ΔE1B19K-deleted mutant and gemcitabine inhibit tumor progression. *A*, animals with PT45 s.c. tumors were treated with the indicated doses (mock = E1A-deleted virus) and tumor growth was monitored. ** $P < 0.01$ and * $P < 0.05$ for combination treatments compared with either single-agent treatment and * $P < 0.05$ for each treatment compared with mock-treated animals. Significance determined by one-way ANOVA analysis. *B*, Kaplan-Meier curves for the indicated treatment groups. All combinations were significantly different from single-agent treatments with ** $P < 0.05$. The percentages of mice free from tumor progression (tumor volume < 500 μL) at each time point were estimated using the Kaplan-Meier method, 6 to 10 animals per group. *C*, immunohistochemistry of representative tumor sections from the studies with viruses at 1 10^6 vp and gemcitabine at 2.5 mg/kg.Three tumors were evaluated from each treatment group; representative micrographs at 100 and 200 magnification for hexon and E1A, respectively.

Europe PMC Funders Author Manuscripts

Table 1

Median time to tumor progression in animals treated with combinations of 1 or 2.5 mg/kg gemcitabine with Ad5ΔE1B19K or Ad5 at 1 10^6 vp

Treatment	Time to progression (median, in d)		
	Virus	Gem 1 mg/kg	Gem 2.5 mg/kg
Gem 1 mg/kg	-	35	-
Gem 2.5 mg/kg	-	-	62
ΔE1A-Ad5	38	nd	65
ΔE1B19K	51	76	>110
Ad5	65	72	82